Resistance to Silver Electrolytic Migration for Thick-Film Conductors Prepared from Mixed and Alloyed Powders of Ag-15Pd and Ag-30Pd

Jing-Chie Lin and Jui-Yu Chuang

Department of Mechanical Engineering, National Central University, Chung-Li, Taiwan 32054

ABSTRACT

Thick-film conductors, made from mixed and alloyed powders of Ag-15Pd and Ag-30Pd, have been explored in distilled water at a bias of 5 V to assess their resistance to electrolytic silver migration. It was found that the resistance increases with the Pd concentration in the thick films (*i.e.*, Ag < Ag-15Pd < Ag-30Pd). The film made from mixed powders is more resistant as compared with that from alloyed powders having the same compositions (*i.e.*, 15A < 15M and 30A < 30M). Based on electrochemical study and analysis of reaction products, the interpretation for the resistance sequence has been discussed.

Introduction

Metallic electromigration has long been recognized as a significant failure mode in many electrical and electronic systems.[1] On the consideration of environmental temperatures and moisture, the electromigration is categorized in two types: electrolytic (ionic), occurred at ambient temperatures (<100°C) in the presence of moisture; and solid-state (electron momentum transfer), occurred at higher temperatures (>150°C) in the absence of moisture. The first type is water dependent and tends to occur whenever the insulator separating the conductors (as on PC boards, flexible circuitry, chip carrier, or IC ceramics) has acquired sufficient moisture to allow electrolytic conduction under a bias of electrical potential.

In the present work, the ionic migration was studied. The metal is dissolved from the positive conductor (anode), transfers through or across a nonmetallic medium, then is deposited and extended from the negative conductor (cathode) to the anode under the influence of an applied electrical field. This metal electrolytic migration eventually produces failures by shorting across the interconductor spacings. Silver is a susceptible metal which readily undergoes electrochemical migration, so that many workers have used the term "silver electrolytic migration" to describe the impairment of Ag-bearing thick films during their application in humid atmosphere.[1-3]

Silver-palladium alloy is better than pure silver for thick-film conductors due to its superior resistance for both electrochemical migration and solder leach.[2,5] However, the addition of palladium increases the cost and is always at the expense of solderability and conductivity. It is common practice, therefore, to produce a range of silver-palladium alloys of different palladium content (5 to 40 weight percent (w/o) so that the best compromise may be chosen for any particular application.[6] The role of palladium on the resistance to Ag electrolytic migration for several Ag-Pd thick films has been investigated in our previous work.[7] It inferred that the resistance increases with Pd concentrations from 5 to 30 w/o in the Ag-Pd thick films.

The electrical properties of thick films depend on the ink ingredients, substrate, and manufacturing process.[2] The effect of the metal component (*e.g.*, Ag-Pd powders) on the properties of Ag-Pd thick-film conductors has been studied.[8,9] Using powders prepared by spray-pyrolysis, Nagashima[8] reported that alloy powders are better than mixture lots in the manufacturing of thick film conductors. On the other hand, using powders made by chemical coprecipitation, one of the authors[9] found that the sintering behavior for thick films prepared from different types (mixed, alloyed, and partially alloyed) was quite different. In this work, the electrolytic silver migration for thick films made from various coprecipitation powders was of interest. The thick films, prepared from mixed and alloyed powders of Ag-15Pd and Ag-30Pd, were investigated to compare their resistance to silver electrolytic migration.

Experimental

Preparation of the thick-film conductors.—All samples of metal powders (Ag, Pd, Ag-15Pd, and Ag-30Pd) employed in this work were produced by chemical coprecipitation. Alloyed powders (15 and 30 A) were prepared via a novel process;[10] pure Ag, pure Pd, and mixed Ag-Pd powders (15 and 30 M) were supplied by ERL, ITRI (Taiwan).[11,12] The powders are spherical and their properties are listed in Table I. The particle size (1.40 to 2.42 μm) and specific surface area (1.14 to 2.00 $m^2 g^{-1}$) for the powders are similar.

Two patterns of thick films were printed on the alumina substrate (96% Al_2O_3) by a sequence of processes described previously.[7] Pattern 1 (Fig. 1a) is a couple of lines; whereas pattern 2 is a single square with an extra tail for wire soldering (Fig. 1b). A wet film 60 μm thick, was kept at ambient for 15 min for leveling, and was dried at 150°C in an infrared furnace for 12 min. These dried prints were then fired in a belt furnace (BTU), wherein the temperature of the heating zone increased to 850°C and then gradually decreased.

Measurement of bridging current in distilled water at 5 V and in situ observation of the silver electromigration.—A specimen with pattern 1 (Fig. 1a) was placed horizontally in a 200 ml cell (cell constant 2.84×10^3 m^{-1}, Fig. 2a), wherein distilled water (conductivity at 230 μS m^{-1}) was filled to cover the specimen at a depth of 2 mm from the water level. The tails of the line couple were soldered to conducting wires (copper) in connection with a potentiostat (EG&G PAR Model 273). An electric field of 5 V was applied between the couple by the potentiostat to measure the current.

Another piece of specimen with pattern 1 (Fig. 1a) was used for *in situ* inspection of silver migration under an optical microscope (Olympus BX 60M). A drop of distilled water was placed on the line couple, across which an electric field of 5 V was applied by the potentiostat and subject to observation. After removal of the bias and evapora-

Table I. Properties of the pure Ag, pure Pd, and Ag-Pd powders from chemical precipitation.

Powder type	Composition (w/o Ag-w/o Pd)	50% particle size (μm)	Surface area ($m^2 g^{-1}$)	Tap density (Mg m^{-3})
Ag	100 Ag	2.42	1.86	1.75
Pd	100 Pd	1.40	1.45	2.20
15M	85Ag-15Pd	1.35	1.14	1.22
15A	85Ag-15Pd	1.60	1.30	1.40
30M	70Ag-30Pd	1.80	2.00	2.10
30A	70Ag-30Pd	2.00	1.50	2.45

tion of the water drop in the ambient, micrographs in better focus were obtained.

Anodic polarization of thick films in 0.01 M NaOH solution.—Figure 2b depicts the cell for the study of potentiodynamic polarization and the measurement of anodic current at constant potentials. Two pieces of specimens with pattern 2 (Fig. 1b) were immersed vertically in the cell at a distance of 20 mm to act as working and counterelectrodes, respectively. A solution of 0.01 *M* NaOH (conductivity at 510 mS m^{-1}) was filled in the cell. The electrode potential was controlled through a Luggin capillary with a mercury-mercurous sulfate electrode (MMSE) by the potentiostat. All the potentials are reported in the normal hydrogen electrode (NHE) scale. All the experiments were performed at room temperature.

Analysis of the thick films and their reaction products.—The morphology for the thick films (print patterns 1 and 2), before and after the electrochemical migration test, was examined by a scanning electron microscope (SEM, JSM-T330, JEOL). The reaction products on both electrodes (cathode and anode) were identified by x-ray diffraction [XRD, Shimadzu XD-5, copper target Cu K (0.15405 nm)]. The anodic film was analyzed by grazing incident x-ray diffraction (GIXD) with an incident angle of 0.30°. Surface analysis of the anodic films was carried out with Auger electron spectroscopy (AES, VG Scientific Instrument MICRO LAB III 310) and electron spectroscopy for chemical analysis (ESCA, MICRO LAB III 310). Auger peak amplitudes were measured as a function of sputtering time. Sputtering was performed with 1 kV argon ions. To convert the time scale into a depth scale, Ta_2O_5 films of known thickness formed anodically on tantalum were employed as internal standard.[13]

Results

Measurement of bridging current.—Figure 3 shows the variation of bridging current as a function of time for several thick films in distilled water at a bias of 5 V. It was seen that the current profile varies with the films made from different powders. In Fig. 3, the bridging current for the film made from pure Ag powders (curve Ag) increases abruptly in 800 s. The films made from the alloyed and mixed powders of Ag-15Pd (curves 15A and 15M) depict a

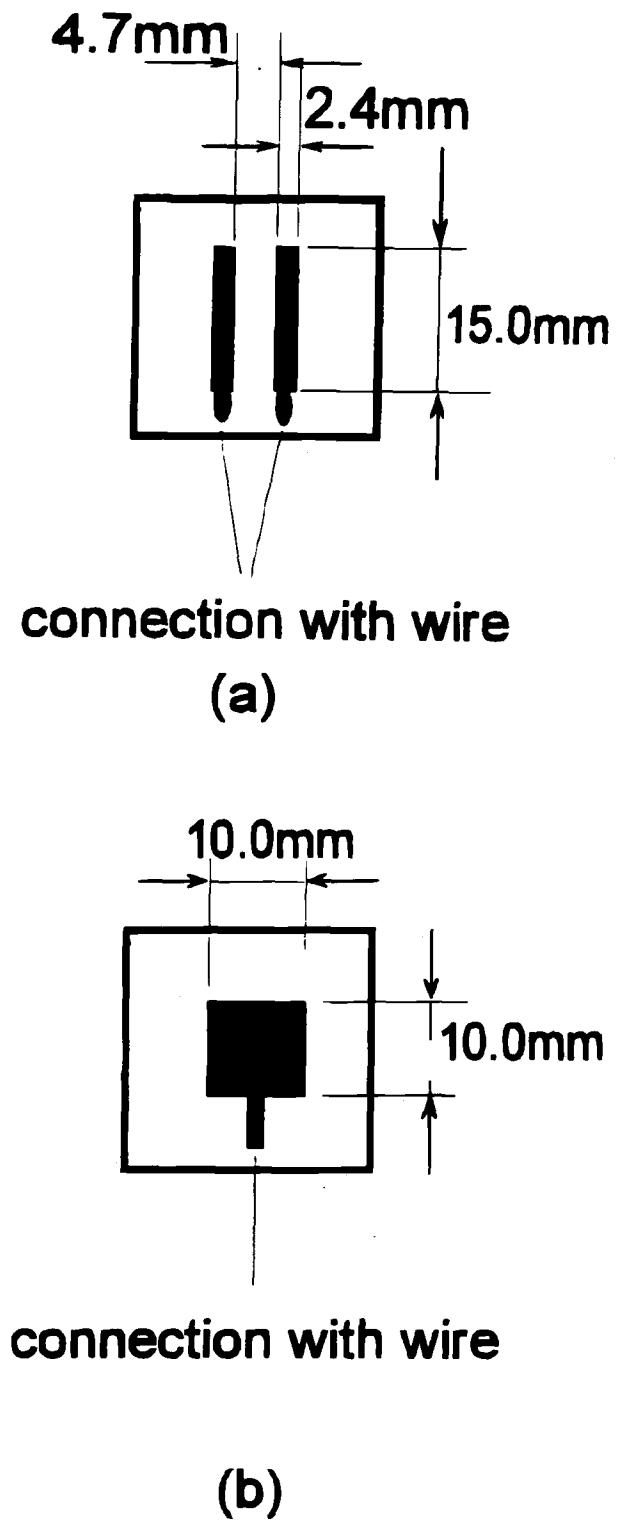

Fig. 1. Print patterns for (a) microscopic observation and measurement of migration current in distilled water at 5 V, and for (b) anodic polarization and examination of film products at various anodic potentials.

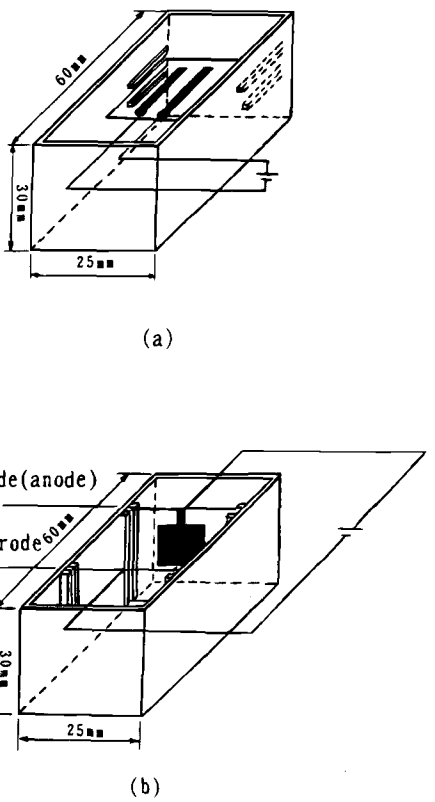

Fig. 2. Electrolytic cells (a) for measurement of electromigration current in distilled water at 5 V, and (b) for anodic potentiodynamic polarization in 0.01 *M* NaOH solution, and for preparation of anodic films in distilled water at 5 V, as well as in 0.01 *M* NaOH at various potentials.

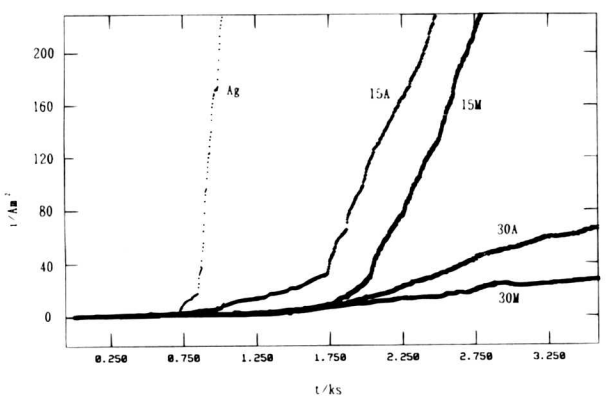

Fig. 3. Variation of current density as a function of time for various thick-film conductors in distilled water at 5 V. Curves Ag for pure Ag; 15A and 15M for the alloyed and mixed Ag-15%Pd; 30A and 30M for the alloyed and mixed Ag-30%Pd, respectively.

two-stage transition on current curves. A small current is preceded at earlier stage which increases steadily with time (*i.e.*, 1750 s for 15A and 2000 s for 15M); it then increases abruptly at later stage. In contrast, the current for the films made from the alloyed and mixed powders of Ag-30Pd (curves 30A and 30M) just increases gradually with time. It shows no sudden increase even at durations longer than 3500 s. Fixing the durations in Fig. 3, the bridging current decreases in the order: Ag > 15A > 15M > 30A > 30M. Obviously, the bridging current decreases with Pd concentrations in the thick films (*i.e.*, Ag > 15A, 15M > 30A, 30M). Moreover, the current is smaller for the film made from mixed powders than that made from alloyed powders having the same composition (*i.e.*, 15A > 15M; 30A > 30M).

Deposits on the cathode.—In situ inspection of the silver electrochemical migration was made microscopically for several thick films in distilled water at 5 V. As obtained in our previous study,[7] the deposits produced on the cathode showed quite different appearances: dendrites (Fig. 4a) on the pure Ag film, cloud-like layers (Fig. 4b and c) on the Ag-30Pd films (30 M and 30 A), and dendrites together with cloud-like layers (Fig. 4d and e) on the Ag-15Pd films (15M and 15A). SEM morphologies indicated that both dendritic and cloud-like products were fabricated by needle-like crystals. The needle crystals in the former were observed to be thicker and denser in contrast to the latter. The dendrite and cloud-like layer were separately collected and they were identified as metal silver by XRD analysis.

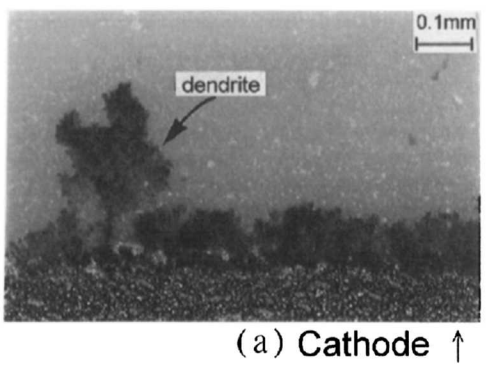

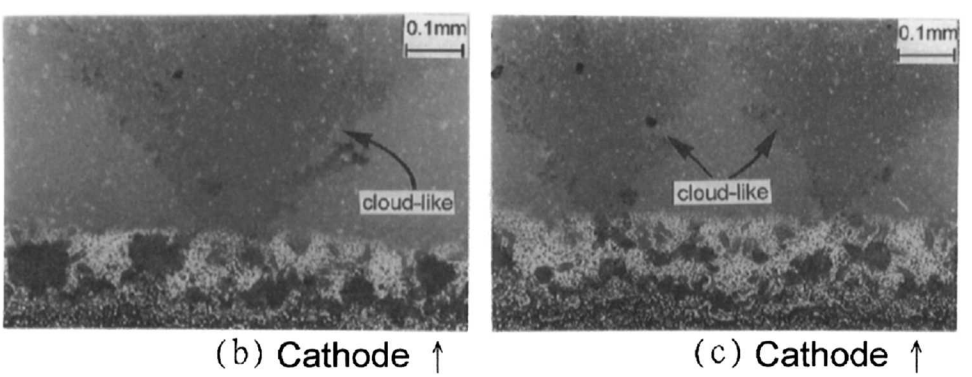

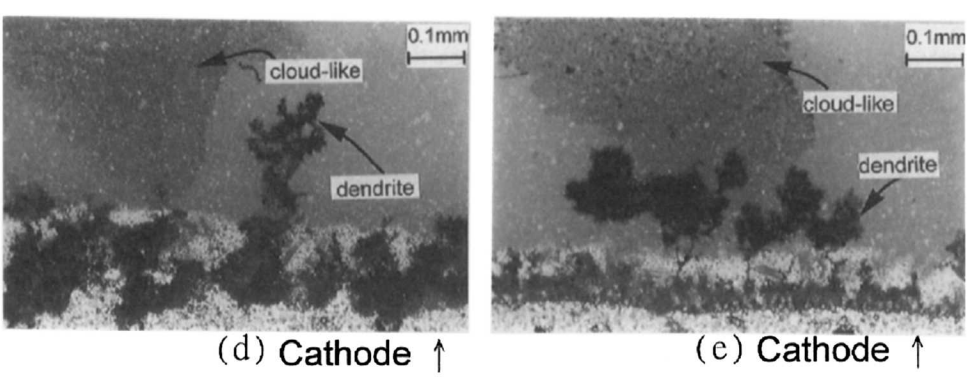

Fig. 4. Optical micrographs for thick films, prepared from the (a) pure Ag, (b) alloyed Ag-30%Pd, (c) mixed Ag-30%Pd, (d) alloyed Ag-15%Pd and (e) mixed Ag-15%Pd powders, in distilled water at 5 V after 250 s.

A correlation was found between the growth rate of the cathodic deposits (shown in Fig. 4) and the current profile shown in Fig. 3. In the case of pure Ag conductors, many dendritic silver filaments were deposited, some of them grew swiftly to bridge the gap between the electrodes. The dendrite is more conductive than the cloudy layer because the former is built up by denser Ag crystals. Rapid growth of the silver dendrites is responsible for the sudden increase of current on curve Ag in Fig. 3. In the case of Ag-30Pd conductors, only sparse cloud-like layers were found between the electrodes. Slow growth of the cloudy layers results in a slight increase of current on curves 30 M and 30 A in Fig. 3. In the case of Ag-15Pd conductors, cloudy layers were formed first, some of them were thickened to become dendrites, then grew swiftly to bridge the electrodes. This phenomenon results in an initially gradual and subsequently rapid increase of the current on both curves 15A and 15M. It was seen that the growth rate is slower for the films made from the mixed powders than from the alloyed powders having the same Pd content. As a result, the current at constant durations shows the series: 15M < 15A and 30M < 30A. In one word, the facility of silver electrolytic migration is determined by the powders from which the thick films are made.

Reaction products on the anode.—ESCA analysis of the reaction products on the anode was made. The anodic products on the films made from pure silver (Ag) and pure palladium (Pd) powders were identified as Ag_2O and PdO alone, respectively. The anodic products on the films made from Ag-15Pd powders were complicated. Figure 5a and b depict the ESCAs of the anodic products, for the films made from the alloyed (15A) and mixed (15M) lots, in distilled water at a bias of 5 V for 2200 s. According to the binding energies reported[14-16] (*i.e.*, 335.4 eV [Pd ($3d_{5/2}$)] and 340.1 eV [Pd ($3d_{3/2}$)] for metal Pd; 336.5 eV [PdO ($3d_{5/2}$)] and 342.2 [PdO ($3d_{3/2}$)] for palladium oxide; 368.2 eV [Ag ($3d_{5/2}$)] for metal Ag; and 367.8 eV [Ag_2O ($3d_{5/2}$)] and 373.8 eV [Ag_2O ($3d_{3/2}$) for Ag_2O], they are composed of metal Pd, palladium oxide, and silver oxide. The intensities of the Pd and PdO peaks are greater for the 15M than the 15A (in Fig. 5a), however, the intensities of the Ag_2O peaks in the former is smaller (Fig. 5b). The area under the peaks corresponding to PdO and Pd (in Fig. 5a) was integrated to estimate their relative amounts. The area ratio of total peak areas between the Pd ($3p_{3/2}$, 531.4 eV) and O (1s, 529.3 eV) is also estimated for confirmation. The ratios of PdO/Pd were found to be 68/32 and 61/39 for the 15M and 15A films, respectively. This result implied that PdO is enriched on the anode of the 15M as compared with that of the 15A. In other words, the anode surface on the 15M film comprises more PdO but less Ag_2O than on the 15A film.

The ESCAs, as shown in Fig. 6, depict that the intensity for the peaks of PdO and Pd on the 30M film is greater than on the 30A film. The ratios of PdO/Pd were calculated to be 81/19 and 73/27 for the 30M and 30A films, repectively. However, it was worth noting that not any Ag_2O peak can be observed on the anode of the 30M and 30A films. The reaction products on the anode are merely PdO and Pd.

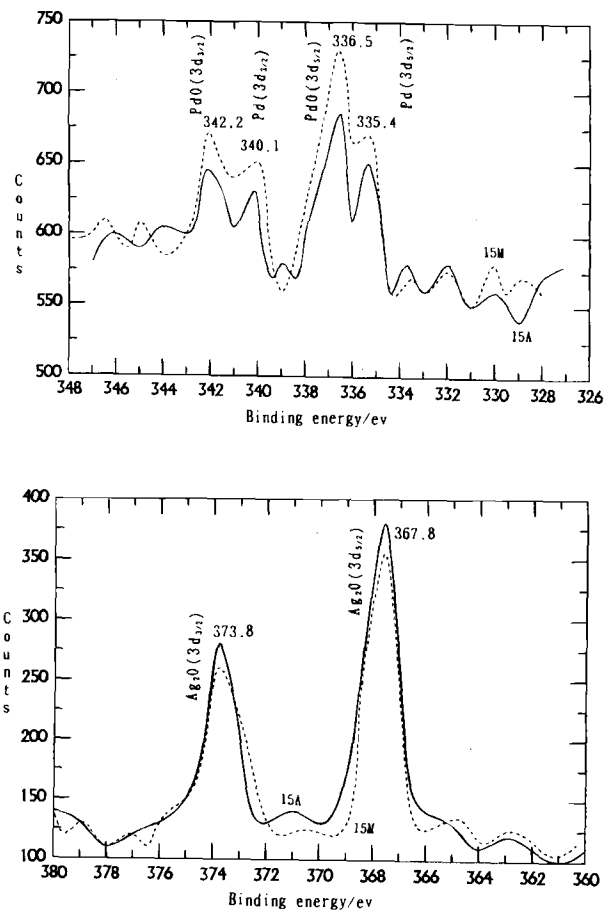

Fig. 5. (a, top) ESCA of Pd and PdO for the anodic films prepared from the alloyed and mixed Ag-15%Pd powders (15A and 15M, respectively) post the test in distilled water at bias of 5 V for 2 200 s; (b, bottom) ESCA of Ag_2O for the anodic films prepared from the alloyed and mixed Ag-15%Pd powders (15A and 15M, respectively) after the test in distilled water at bias of 5 V for 2200 s.

Discussion

According to the definition of electrolytic silver migration, the migrating silver originates from the anode of the Ag-Pd thick films. Evidently, the facility of silver dissolution from the anode may affect the susceptibility of the thick films to silver electrochemical migration. A realization of anodic behaviors for various thick films should be helpful to discern their resistance to silver electrochemical migration. For preventing the interference of IR drop, the anodic polarization was conducted in a solution of 0.01 *M* NaOH instead of distilled water. Preliminary tests indicated that the phenomenon of silver electromigration in distilled water is much like that in 0.01 *M* NaOH, rather than in 0.01 *M* H_2SO_4 (or 0.01 *M* HNO_3) solutions.

Potentiodynamic polarization of the anode.—For thick films varying in Pd concentrations.—Figure 7 depicts the anodic potentiodynamic polarization, for thick films containing various Pd concentrations, in the 0.01 *M* NaOH solution. The current peaks for the pure silver film (curve Ag) are virtually the same as those found in the literature.[7,17,18] The product of the peaks 0.200 and 0.365 V has

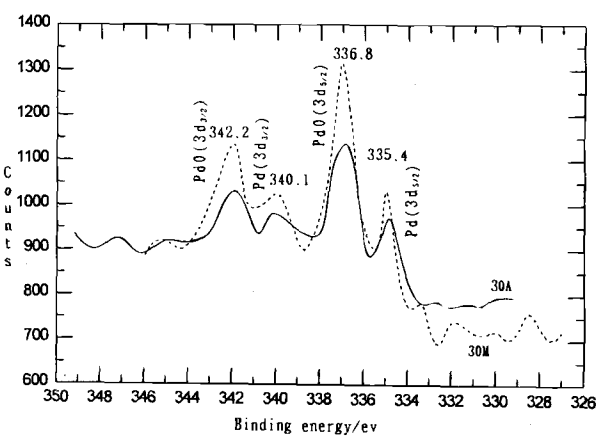

Fig. 6. ESCA of Pd and PdO for the films prepared from the alloyed and mixed Ag-30%Pd powders (30A and 30M, respectively) after the test in distilled water at bias of 5 V for 2200 s.

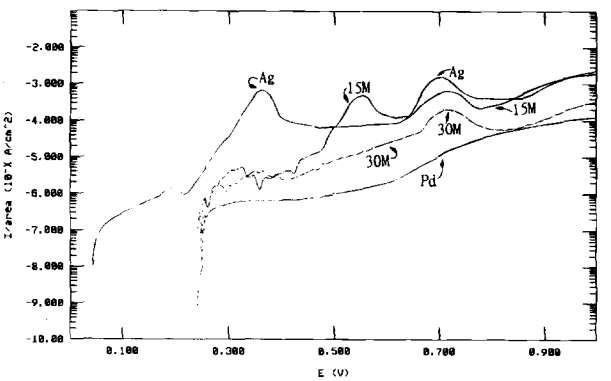

Fig. 7. Anodic potentiodynamic polarization for the thick films in 0.01 *M* NaOH solution. Curves Ag and Pd represent the films made from the pure Ag and pure Pd powders, respectively; curves 15M and 30M represent the films made from the mixed powders of Ag-15%Pd and Ag-30%Pd, respectively.

been suggested to be Ag_2O from Ag, and the peak 0.702 V to be AgO from Ag_2O. Samples of the pure Ag were exposed for 1800 s, at constant potentials, in a 0.01 *M* NaOH solution, and then the surface film was analyzed with ESCA. At 0.365 V, the surface of the sample showed Ag_2O as a corrosion product. At 0.702 V, a thin film of AgO was detected over the Ag_2O layer. As the difference between the ESCA peak for Ag_2O and that for AgO is less than 0.1 eV, it was not possible to measure the depth of the AgO layer.

Examining the curve Ag in Fig. 7, the anodic current increases steeply with increasing the potentials from 0.044 (the rest potential) to 0.365 V. This phenomenon is responsible for silver dissolution from the pure Ag film, governed by[17,18]

$$Ag \rightarrow Ag^+ + e^- \quad E^\circ = 0.799 + 0.0591 \log (Ag^+) \qquad [1]$$

At potentials higher than 0.365 V, the silver in the pure Ag film undergoes the reaction

$$Ag + \tfrac{1}{2}H_2O \rightarrow \tfrac{1}{2}Ag_2O + H^+ + e^-$$

$$E^\circ = 1.173 - 0.0591\ pH \qquad [2]$$

to form Ag_2O, which is then subject to further oxidation by

$$Ag_2O + H_2O \rightarrow 2AgO + 2H^+ + 2e^-$$

$$E^\circ = 1.398 - 0.0591\ pH \qquad [3]$$

at potentials higher than 0.702 V. Two current plateaus were found on the curve Ag, the first (at 0.380 to 0.680 V) is related to pseudo-passivation by Ag_2O, and the second (at 0.720 to 0.880 V) ascribed to incomplete passivation by AgO.[17,18] Hamilton *et al.*[19] confirmed the chemical nature and the formation potential of both oxides through Raman spectroscopy.

When palladium was involved to make an Ag-Pd thick film, the rest potential was observed to shift at higher potentials (roughly at 0.247 V for the Ag-15%Pd, Ag-30%Pd, and Pd films). In the meantime, the polarization curve introduces an extra hump at 0.300 to 0.450 V and changes the profile. In addition to the current hump, curve 15M in Fig. 7 displays two peaks at 0.553 and 0.715 V, however, curve 30M exhibits only a single peak at 0.717 V. Samples of the Ag-15Pd and Ag-30Pd were exposed for 1800 s, at constant potentials, in a 0.01 *M* NaOH solution, and then the surface film was analyzed with ESCA. At 0.400 V, the surface of both samples showed PdO as a corrosion product, and no silver compounds were detected. Thus, the small current hump is due to the PdO layer. At 0.650 V, Ag_2O and PdO as the corrosion products for the Ag-15Pd whereas only PdO was detected for the Ag-30Pd. At 0.800 V, a thin film of AgO was detected above the Ag_2O and PdO layers on both the specimens.

The polarization curve of the pure Pd thick film (curve Pd) was shown in Fig. 7 to discern the role of Pd on the anodic behavior of the Ag-Pd thick films. A typical passivation due to the effect of a PdO layer (also detected by ESCA) is obtained, according to the following reaction[20,21]

$$Pd + H_2O \rightarrow PdO + 2H^+ + 2e^- \quad E^\circ = 0.896 - 0.0591\ pH \qquad [4]$$

The equilibrium potential, calculated from Eq. 4 in the 0.01 *M* NaOH solution (pH close to 12), is 0.188 V. The rest potential was observed to be greater than the equilibrium potential. Thus, PdO film is promptly formed on the surface of pure Pd thick film to passivate itself. The anodic current is much lower for the pure Pd film at passive potentials than for the pure Ag film at pseudo-passive potentials (*i.e.*, $10^{-6} << 10^{-4}$ A cm^{-2}). Hence, the PdO film is more protective that the Ag_2O and AgO films. This result is consistent with the electrochemical thermodynamics of the palladium and silver.[22,23]

By using Eq. 2 through 4, the potentials for the oxide formation are calculated and compared in the solutions at pH 12, 7, and 2. They are: 0.187 for PdO, 0.464 for Ag_2O, and 0.689 V for AgO at pH 12; 0.482 for PdO, 0.759 for Ag_2O, and 0.984 V for AgO at pH 7: 0.779 for PdO, 1.055 for Ag_2O, and 1.280 V for AgO at pH 2. The potential shift of Ag_2O and AgO, in comparison the calculated data with those observed on curve Ag in Fig. 7, may be ascribed to structural differences between thick film and pure metal. Nevertheless, palladium is more susceptible to oxidation than silver if they coexist. As a result, formation of PdO on the anode is prior to Ag_2O. In the presence of this protective PdO layer, the sublayer silver component in the Ag-Pd alloys is less susceptible to dissolution in the humid environment. The anodic current corresponding to silver dissolution becomes smaller, and the Ag_2O peak occurs at higher potentials.

In the Ag-Pd thick films containing 5-15%Pd, the coverage on the anode by PdO layer is not sufficient, the exposed silver component is selectively dissolved and then oxidized. The polarization curve depicts a small PdO hump and the Ag_2O and AgO peaks. Increasing the Pd from 5 to 15% in the thick films, the anodic coverage of PdO increases, and the silver dissolution is more difficult. The Ag_2O peak delays to higher potentials. However, the AgO peak remains nearly unchanged. This is consistent with the result of our previous study.[7] Further increasing the Pd concentration up to 20 to 30 w/o, the anodic coverage by the PdO is sufficient, the silver can only dissolve at higher potentials where PdO layer become less protective. Thus the dissolution current is much lower and the oxidation of silver to Ag_2O is delayed to much higher potentials. At such a high potential, as soon as the Ag_2O forms, it oxidized further to become AgO. As a result, the Ag_2O peak is delayed and combines with the AgO to form a single peak at 0.750 V. This result was confirmed with the analysis of anodic film by ESCA at various potentials.

For thick films made from different types of powders with constant Pd concentrations.—Figure 8 displays the polarization curve for thick films made from different types of powders. The rest potentials showed the order 15A < 15M < 30A < 30M, even in a slight difference. All the curves in Fig. 8 show the presence of PdO hump, and confirm the result of Fig. 7 that the anodic current decreases with the Pd contents in the thick films (*i.e.*, 30A, 30M < 15A, 15M). In addition, the polarization curves in Fig. 8 show a potential shift for the films made from the powders having a constant composition but in different types. The film made from 15A exhibits the Ag_2O peak at 0.527 and AgO peak at 0.735 V. In contrast, the film made from 15M shows a higher Ag_2O peak (0.553 V), whereas a lower AgO peak (0.715 V). Increasing the potential from the rest potentials of the specimens, the 15A film is more susceptible to form Ag_2O than is the 15M film, whereas the transition from Ag_2O to AgO is less readily. At potentials below

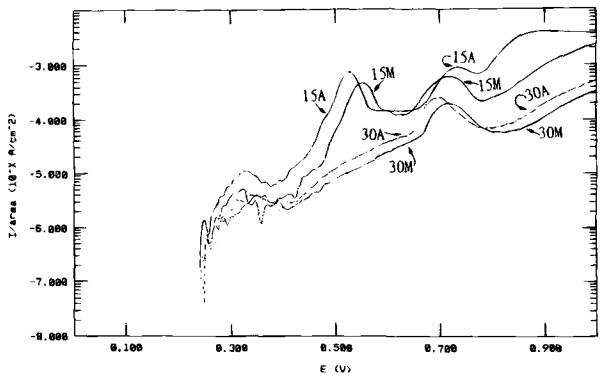

Fig. 8. Anodic potentiodynamic polarization for the thick films in 0.01 *M* NaOH solution. Curves 15A and 15M represent the films made from the mixed and alloyed Ag-15%Pd, whereas curves 30A and 30M represent the films made from the mixed and alloyed Ag-30%Pd, respectively.

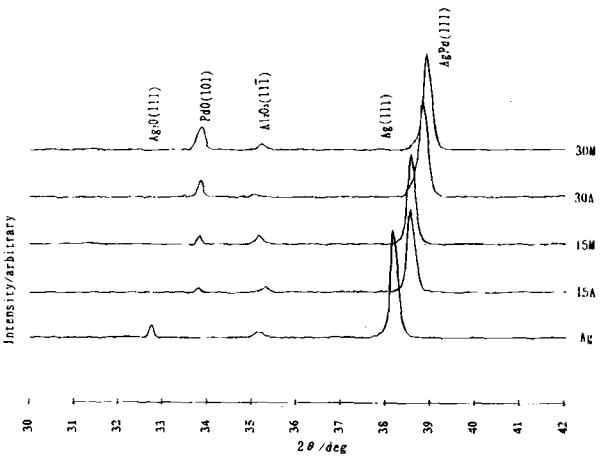

Fig. 10. Grazing incident x-ray diffraction patterns for the anode in a couple of thick films made from the pure silver (Ag), the alloyed and mixed Ag-15%Pd (15A and 15M), the alloyed and mixed Ag-30%Pd (30A and 30M) after the test in 0.01 *M* NaOH solution at 0.400 V for 800 s.

0.520 V and above 0.680 V, smaller anodic current was observed for the 15M film than the 15A film. With regard to polarization curves for the Ag-30Pd thick films, the 30A and 30M films show a single peak at 0.700 and 0.717 V, respectively. At potentials below 0.715 and above 0.800 V, curve 30M shows a smaller anodic current than curve 30A at the corresponding potentials. As a result, in a wide range of potentials, the films made from mixed powders inclined to obtain lower anodic current than those from alloyed powders having the same composition. Additional evidences are provided in the following.

Anodic current at constant potentials for the thick films in the 0.01 M NaOH.—At potentials lower than 0.500 V.— Anodic current for thick films was measured against time at constant potentials such as 0.300, 0.400, 0.500, 0.530, 0.600, 0.700, 0.800, and 0.900 V in the cell shown in Fig. 2. Figure 9 shows the typical *i-t* plot for several thick films at 0.400 V. All the current curves decrease abruptly with time, especially in the cases of 15A, 15M, 30A, and 30 M. The anodic current is much smaller for the Ag-Pd thick films than for the pure silver film. At 0.300 V, it is incapable of distinction the *i-t* curves for the individual Ag-Pd films (*i.e.*, the current order: 30M ≈ 30A ≈ 15M ≈ 15A < Ag at a duration of 200 s). At 0.400 V, the current curves for the Ag-Pd thick films were somewhat different in the order 30M ≈ 30A ≈ 15M < 15A < Ag at a duration of 200 s. Figure 10 shows the GIXDs for the anodic films produced on various thick films which had been controlled at 0.400 V in 0.01 *M* NaOH solution for 1800 s. Ignoring the peaks for alumina substrate and original metallic films (Ag or AgPd), a single Ag_2O peak was observed on the pure Ag specimen, and a single PdO peak on the Ag-Pd specimens (15A, 15M, 30A, and 30 M). This fact confirms that the presence of PdO layer inhibits the silver dissolution and moves the Ag_2O formation to higher potentials.

At potentials between 0.500 and 0.700 V, and higher than 0.700 V.—Figure 11 shows the *i-t* curves for the thick films at 0.530 V. The anodic current decreases rapidly in 100 s to several levels and then shows different variations with times. The anodic current displays the order 30M < 30A < 15M < 15A < Ag, and the current for the 30M and 30A films (as well as 15M and 15A films) is near the same at durations longer than 1000 s. Figure12 shows the GIXDs for the anodic products produced at 0.530 V. It was found that Ag_2O peak is present on both the pure Ag and 15A films, whereas it is absent on the other specimens. The PdO peak was found on all the AgPd specimens. The intensity of the Ag_2O peak is smaller for the 15A than for the pure Ag. However, the intensity of the PdO peak increases in the series 15A < 15M < 30A < 30 M. Examining the GIXDs for the anodic products produced at 0.650 V, it displays an additional Ag_2O peak on the 15M film, as compared with Fig.12. This fact infers that the oxidation of silver in the 15M film happens at higher potentials than that in the 15A film. Exploring the reaction products, the ones produced

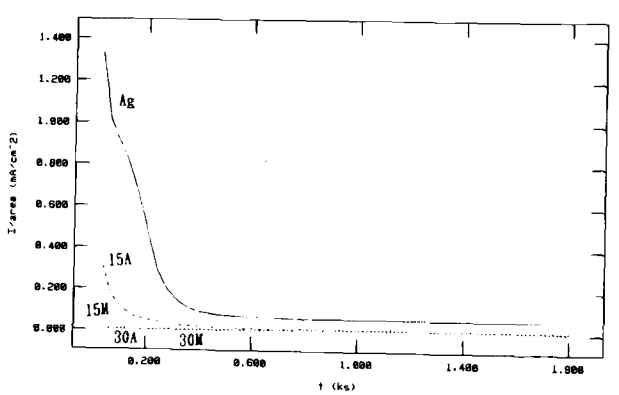

Fig. 9. Anodic current density as a function of time for several thick films in 0.01 *M* NaOH solution at 0.400 V. Curves Ag for the film made from pure Ag; 15A and 15M for the films made from alloyed and mixed Ag-15%Pd; 30A and 30M for films made from alloyed and mixed Ag-30%Pd, respectively.

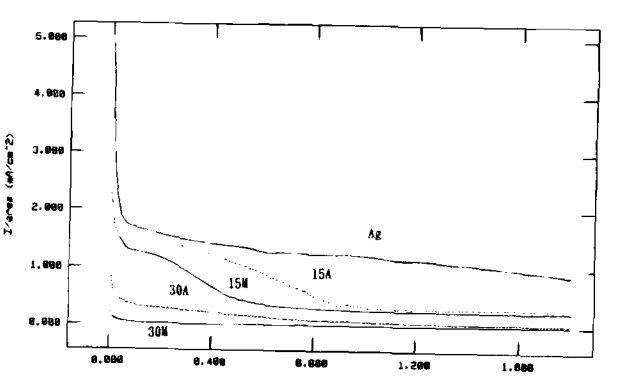

Fig. 11. Anodic current density as a function of time for several thick films in 0.01 *M* NaOH solution at 0.530 V. Curves Ag for the film made from pure Ag; 15A and 15M for the films made from alloyed and mixed Ag-15%Pd; 30A and 30M for films made from alloyed and mixed Ag-30%Pd, respectively.

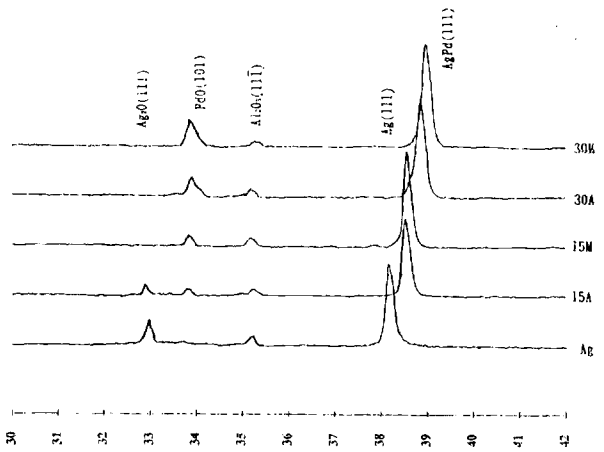

Fig. 12. Grazing incident x-ray diffraction patterns for the specimens (Ag for pure Ag, 15A and 15M for Ag-15%Pd alloy and mixture, 30A and 30M for Ag-30%Pd alloy and mixture, respectively) after the test in 0.01 *M* NaOH solution at 0.530 V for 800 s.

on the anode of thick films in 0.01 *N* NaOH solution at 0.400 to 0.650 V are quite similar to those produced on the corresponding specimens in the distilled water at a bias of 5 V.

The *i-t* plot for the thick films at 0.600, 0.700, 0.800, and 0.900 V was found to be similar to Fig.11 except the current amplitude becoming greater. Figure 13 shows the GIXDs for the anodic products produced on various thick films at 0.730 V for 1800 s. Both silver oxides (Ag_2O and AgO) were formed on the pure Ag, 15A and 15M films, and one PdO peak on the 15A, 15M, 30A, and 30M films. Exploring the GIXDs for the anodic products produced at potentials greater than 0.800 V, the Ag_2O and AgO peaks were both observed even on the 30A and 30M films, their intensity increases with potentials and durations. The analysis of ESCA on the anodic films of various thick films confirmed the results of GIXD.

Metallurgical aspect for the interpretation of the resistance series.—The mechanism of silver electrolytic migration in pure Ag thick films has been well known.[1,3,4] In regards to silver-palladium thick films, the resistance to silver electrolytic migration increases with the Pd concentrations in the films. Due to electrochemical studies, coverage of the PdO layer plays an important role on the silver dissolution from the anode of the thick films. The anodic coverage of the PdO is proportional to the Pd contents in the thick film. The more concentrated Pd in thick films the higher possibility of it to be oxidized, and the greater is the coverage on the anode. As blocked by the PdO layer, the silver in the anode of Ag-Pd thick films dissolves less readily, and results in diluted silver concentrations in the electrolyte as compared with the case of the pure Ag films. The depletion of silver ions in the electrolyte slows the silver deposition on the cathode. Hence the resistance to silver electrolytic migration is enhanced. Thus, the model of anodic coverage by the PdO is satisfactory to explain the resistance series: Ag < Ag-15Pd < Ag-30Pd.

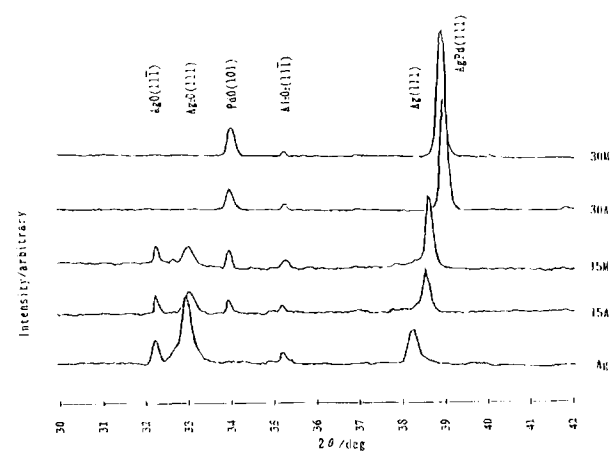

Fig. 13. Grazing incident x-ray diffraction patterns for the anode in a couple of thick films made from the pure silver Ag), the alloyed and mixed Ag-15%Pd (15A and 15M), the alloyed and mixed Ag-30%Pd (30A and 30M) after the test in distilled water at 0.650 V for 1800 s.

The metallurgical aspect is also considered to understand why the resistance is higher for the 15M film than the 15A film (and for the 30M film than the 30A film). The structure of the films as sintered at 850°C was examined. The films made from the alloyed powders are sintered by means of direct coalescence of the alloy particles to develop a simple polycrystalline alloy film. In contrast, the films made from the mixed powders are sintered in complicated processes to form a film in layers, incorporated with surface polycrystals of Ag-Pd alloy covered a thin silver matrix onto the substrate. The silver particles in the mixed powders diffuse not only to form a thin silver layer at the interface nearby the substrate, but also to alloy the palladium particles on the thick-film surface. The sintering behavior is beyond the scope of this study, and the detail is discussed in our previous study.[9] In the case of mixed powders sintering, silver diffusion to the substrate leads to Pd-enrichment on the surface of the films made from 15M (and 30M) than the 15A (and 30A).

Checking with AES analysis, the values of the amplitude ratio Pd/Ag on the surface of the sintered thick films show the order: 0.18 (15A) < 0.26 (15M) < 0.43 (30A) < 0.61 (30M). Through analysis with ESCA, the films as sintered were observed to comprise mainly Pd and Ag. However, they turned out to be comprise various oxides, depending on the applied potentials, after being anodically controlled. This confirms the fact that the films made from mixed powders lead to Pd-enrichment on the surface than those made from the alloyed powders having the same composition. The enrichment of Pd results in greater anodic coverage of PdO. Consequently, the resistance to silver electrolytic migration is higher than for the films made from the mixed powders than those made from the alloy having the same composition.

Conclusions

1. The resistance to silver electrolytic migration for thick-film conductors was estimated by means of bridging current measurement in distilled water at a bias of 5 V. The films were observed to be more resistant if they were made from the powders containing higher Pd contents, or from the mixed lots as compared with the alloyed lots in which the Pd contents are the same. Consequently, the resistance shows in the order: Ag < 15A < 15M < 30A < 30M.

2. In the presence of moisture and electrical bias, the cathodic deposition of migrating silver varied its appearance depending on the kinds of thick films: dendrites on the pure Ag film, cloud-like layers on the Ag-30Pd films (30M and 30A), and dendrites together with cloud-like layers on the Ag-15Pd films (15M and 15A). The growth of the cathodic deposits was correlated with the development of silver electrolytic migration.

3. Surface analysis indicated that the resistance of silver-palladium thick films to silver electrolytic migration is ascribed to formation of PdO on the anode. The more readily the formation of PdO, the more resistant is the thick film to silver electrochemical migration.

4. Potentiodynamic study for various Ag-Pd thick films in 0.01 *M* NaOH solution is helpful in understanding their resistance to silver electrolytic migration. Formation of the PdO occurs more readily than that of th Ag_2O. In the presence of protective PdO layer, the anode is so passivat-

ed that the silver component is inhibited to undergo dissolution. Thus, silver electrolytic migration is more resistant for the thick films, which were made from Ag-Pd powders containing higher Pd contents, and from mixed lots having the same Pd contents as the alloyed lots. The inference was confirmed by the measurement of anodic current at constant potentials, and the analysis of reaction products on the anode.

Acknowledgment

The financial assistance provided by the National Science Council of the Republic of China under Contract NSC 83-0405-E008-002 is gratefully appreciated. The authors also would like to thank Huei Hsing Yen of MRL, ITRI, Chu-Tung, Taiwan, for his help with AES and ESCA analyses.

Manuscript submitted Aug. 23, 1996; revised manuscript received Jan. 3, 1997.

National Central University assisted in meeting the publication costs of this article.

REFERENCES

1. S. J. Krumbein, *IEEE Trans. Comp. Hybrids, Manuf. Technol.*, **CHMT-11,** 5 (1988).
2. R. W. Vest, *Ceram. Bull.*, **65,** 631 (1986).
3. T. Kawanobe and K. Otsuka, *IEEE Trans. Comp. Hybrids, Manuf. Technol.*, **CHMT-781,** 220 (1982).
4. H. M. Naguib and B. K. MacLaurin, *ibid.*, **CHMT-2,** 196 (1979).
5. J. Savage, in *Handbook of Thick Film Technology*, P. J. Holmes and R. G. Loasby, Editors, p.107, Electrochemical Pub. Ltd, Scotland (1976).
6. J. R. Larry, R. M. Rosenberg, and R. O. Uhler, *IEEE Trans. Comp. Hybrids, Manuf. Technol.*, **CHMT-3,** 211 (1980).
7. J. C. Lin and J. Y. Chan, *Mater. Chem. Phys.*, **43,** 256 (1995).
8. K. Nagashima, T. Himeda, and A. Kato, *J. Mater. Sci.*, **26,** 2477 (1991).
9. J. C. Lin and W. Wu, *Mater. Chem. Phys.*, **40,** 110 (1995).
10. J. C. Lin, Y. B. Ten, and S. L. Lee, U.S. Pat. 5,514,202 (1996).
11. J. C. Lin, C. S. Jen, and J. K. Du, R.O.C. Pat. Invention No. 50940 (1991).
12. C. S. Jen and T. C. Chaou, R.O.C. Pat. Invention, No. 64254 (1993).
13. H. J. Mathieu and Landolt, *Surf. Interf. Anal.*, **5,** 77 (1983).
14. K. S. Kim, A. F. Gossmann, and N. Winograd, *Anal. Chem.*, **46,** 197 (1974).
15. T. L. Barr, *J. Phys. Chem.*, **82,** 1801 (1978).
16. S. W. Gaarenstroom and N. Winograd, *ibid.*, **67,** 3500 (1977).
17. M. L. Teijelo, I. R. Viche, and A. J. Arvia, *J. Electronanal. Chem.*, **162,** 207 (1984).
18. N. Sato and Y. Shimizu, *Electrochim. Acta*, **18,** 567 (1973).
19. J. C. Hamilton, J. C. Farmer, and R. J. Anderson, *This Journal*, **133,** 739 (1986).
20. J. F. Llopis and F. Collom, in *Encyclopedia of Electrochemistry of the Elements*, Vol. VI, A. Bard, Editor, p. 254, Marcel Decker, New York (1976).
21. G. S. Duffo and J. R. Galvele, *Corros. Sci.*, **34,** 79 (1993).
22. M. Poubaix, in *Atlas of Electrochemical Equilibrium in Aqueous Solutions*, p. 358, Pergamon Press, Oxford (1966).
23. M. Poubaix, *ibid.*, p. 393.
24. S. S. Cole, Jr., *J. Am. Ceram. Soc.*, **68,** C-106 (1985).

Displacement Deposition of Sn from Fluoride Solutions on Pd Predeposited (100) Si Substrate

C. Longo,[a] P. T. A. Sumodjo,[b] and F. Sanz*[,a]

[a]*Departament de Química-Física, Universitat de Barcelona, 08028 Barcelona, Spain*
[b]*Instituto de Química, Universidade de São Paulo, 05599 São Paulo, Brazil*

ABSTRACT

Displacement deposition of tin on Si from fluoride solutions results only in small scattered grains on the surface. However, deposition on a Pd predeposited Si substrate greatly increases the amount of deposited tin. Using morphological and chemical surface analysis, we conclude that Sn deposition occurs on the surface of the substrate placed in between the previously deposited Pd grains. Depending on the distribution of the Pd nuclei on the substrate, a complete surface coverage by nanometric particles of metallic tin can be achieved.

Introduction

The electroless deposition techniques are widely used in semiconductor industries to implement electronic devices. Metal deposition on the surface of the substrate occurs via the electron transfer between the corresponding metal ion and a reducing agent present in the solution, like hypophosphite, hydrazine, or formaldehyde.[1]

Plating of a selected group of metals on silicon substrates can be performed in a different way, using only the corresponding metal ions in fluorinated aqueous solution. In this case, fluoride species (HF, $[HF_2]^-$, and F^-) keep the surface free of silicon oxide, and the cathodic metal deposition is achieved due to simultaneous silicon oxidation.[2-9] This deposition process, also called galvanic displacement, occurs according to the half-cell reactions

$$[SiF_6]^{2-} + 4e = Si + 6F^- \quad [1]$$

$$M^{n+} + ne = M \quad [2]$$

This plating process guarantees high purity of the deposits because it allows a permanent cleaning control of the semiconductor surface. For this reason, as well as the low cost and simplicity of the method, interest in this process has increased. It is known today that deposition becomes effective for Au, Pt, Pd, Cu, and Ni but not for Fe, Cr, Zn, Al, or for Sn.[2-12]

Our work has shown that tin deposition from hydrogen-fluoride solutions can be successfully performed on a palladium predeposited silicon substrate. The predeposition of Pd (also from HF solutions) has been used intensively in order to activate semiconductor or metal surfaces before proceeding to the electroless metal deposition.[5,6,13-18] Recently, we have studied the first stages of displacement deposition from fluoride solutions of some noble metals.[19-22] While trying to deposit tin, and in spite of the relatively concentrated plating solutions, we obtained just small scattered grains on the surface. The presence of predeposited Pd nuclei on the same substrate, however, greatly induced tin deposition. Similar phenomena in a different

* Electrochemical Society Active Member.